VOLUME 8 (SPECIAL ISSUE) 2022

ISSN 2454-3055

Manuscripts under Special issue are published with the Theme
"Modern Perspectives of Biological Sciences"

Guest Editor: Dr. S. Mohanasundaram
Assistant Guest Editor: Dr. S.S. Syed Abuthahir

INTERNATIONAL JOURNAL OF ZOOLOGICAL INVESTIGATIONS

Forum for Biological and Environmental Sciences

Published by Saran Publications, India

International Journal of Zoological Investigations Vol. 8, Special Issue, 275-284 (2022)

International Journal of Zoological Investigations
Contents available at Journals Home Page: www.ijzi.net
Editor-in-Chief: Prof. Ajai Kumar Srivastav
Published by: Saran Publications, Gorakhpur, India

ISSN: 2454-3055

Mathematical Model of Blood Flow through Capillaries to Study Transport of Nanoparticles Using Power Law Fluid Model

Mallik Basu B.* and Garain D.N.

University Department of Mathematics, S.K.M. University, Dumka 814110, Jharkhand, India

**Corresponding Author*

Received: 20th August, 2022; **Accepted:** 27th October, 2022; **Published online:** 17th November, 2022

https://doi.org/10.33745/ijzi.2022.v08i0s.034

Abstract: A model of blood capillary flow that is axially symmetric with a peripheral layer and wall slip is provided mathematically in this study. Power law fluid was employed in the core area of suspension of all erythrocytes whereas Newtonian fluid was used in the periphery plasma layer to analyse longitudinal transport of nanoparticles within blood vessels. The capillary walls are impenetrable to nanoparticles in our study, and they are not absorbent. The formulas for the velocity profile, flow rate, mean velocity, and solute concentration were produced, and the findings were discussed using graphs.

Keywords: Nanoparticles, Power law fluid, Peripheral layer, Erythrocytes, Slip velocity

Citation: Mallik Basu B. and Garain D.N.: Mathematical model of blood flow through capillaries to study transport of nanoparticles using power law fluid model. Intern. J. Zool. Invest. 8(Special Issue): 275-284, 2022.

https://doi.org/10.33745/ijzi.2022.v08i0s.034

Introduction

During recent years, scientific research and technology development have focused on the movement and transport of nanoparticles in small blood vessels. The study of blood flow through blood vessels is essential for understanding the description of the structure and functioning of a living being. The pathophysiology of many arterial illnesses is linked to the features of blood flow and the activity of blood vessel walls. The walls of the vessel can be elastic, moveable, or porous. As a result, it is necessary to grasp the basic mechanics of fluids in order to comprehend the mechanics of blood circulation. The behaviour of blood flow through the vessels of living organisms' circulatory systems has been the subject of numerous theoretical and experimental endeavours. Blood is no longer an uniform viscous fluid in narrow veins. When blood passes through capillaries, it splits into two phases: a Newtonian fluid in the plasma's cell-free layer and a non-Newtonian power law fluid in the plasma's centre core area of erythrocyte suspension.

Nanofluids are now considered an active study area among scientists. In reality, because nanoparticles are extremely selective, efficient, and swiftly internalised by target cells, in a variety of industries for fluid dynamics to function properly, it is essential that nanoparticles be transported longitudinally. They kill unhealthy cells and bind the target region by successfully delivering medicine in small blood channels such as capillaries. The size and concentration of nanoparticles in a base fluid determine their capillary efficiency.

Many researchers have investigated the difficulties of non-Newtonian fluids in fluid flow utilising nanoparticles under various conditions. Gentile *et al.* (2008) and Kirkeeide *et al*. (1977) used a Casson-like fluid model to investigate the blood's longitudinal nanoparticle transport. They talked about the importance of blood rheology and vascular permeability. Ellahi *et al*. (2014) worked at the flow of nanofluid via an artery that had composite stenosis as well as porous walls. Several researchers have addressed various features of artery blood flow analysis. The varied characteristics of blood flow in stenosed arteries have been examined by Mekheimer and El-kot (2012). A number of publications claim that understanding the cardiovascular system's impact requires an examination of blood flow and its properties (Caro *et al*., 1971; Mishra and Shit, 2007; Sandeep and Shine, 2021). At low shear rates, blood, as a suspension of cells, behaves like a non-Newtonian fluid (Charm and Kurland, 1965; Lee, 1974; Shukla *et al.* 1980). By considering the velocity slip condition at the artery wall, Misra and Shit (2007), established mathematical models for blood flow. Mostafa (2011) investigated at how slip velocity affected a non-Newtonian Power-law fluid over a moving surface that was generating heat (Ravelin *et al*., 2009). The purpose of this research was to look at the impact of the peripheral layer and the slip condition on nanoparticle transport in capillaries. We also looked at how the power law index affects nanoparticle velocity and concentration in a base fluid.

Power Law:

The Ostwald-de Waele connection, commonly known as Power Law fluid is a Newtonian fluid whose shear stress is given by-

$$\tau = K\left(\frac{\partial u}{\partial y}\right)^n$$

Where the flow consistency index is denoted by the letter K. (SI units Pa s); the shear rate, sometimes called the velocity gradient perpendicular to the shear plane, is denoted by $\frac{\partial u}{\partial y}$ and measured in SI units per second; the flow behaviour index is n (dimensionless).

As a function of the shear rate, the quantity $\mu_{eff} = K\left(\frac{\partial u}{\partial y}\right)^{n-1}$ represents an apparent or effective viscosity. The graph of log (μ_{eff}) and log ($\frac{\partial u}{\partial y}$) can be used to find the values of K and n. The slope line provides the value of n-1, which can be used to compute n. The value of K is determined by the intercept at log ($\frac{\partial u}{\partial y}$) = 0

Even though it only closely resembles the behaviour of a genuine non-Newtonian fluid, this mathematical expression, sometimes referred to as the Ostwald-de Waele power legislation, is helpful due to its clarity. If n is smaller than one, the power law predicts that effective viscosity will decline endlessly as the shear rate increases, a fluid that has an infinite viscosity at rest and a viscosity of zero as the shear rate approaches infinity is required. A genuine fluid, on the other hand, has an upper and lower limits effective viscosity that are established at the molecular level by physical chemistry. As a result, the power law provides only a good representation of fluid behaviour throughout the shear rate range for which the coefficients were fitted. Other models exist that effectively reflect the entire flow characteristics of shear-dependent fluids, but they are more complicated, consequently, the power law is still utilised to delineate fluid behaviour, produce mathematical hypotheses, and link experimental findings.

Depending on the value of their flow behaviour index, power-law fluids can be divided into three distinct classes (Table 1).

Table 1: Classes of fluid

n	Type of fluid
<1	Pseudoplastic
= 1	Newtonian Fluid
>1	Dilatant

Mathematical Formulation of the Problem:

In a cylindrical coordinate system (r, z), a capillary of radius Re and length l with an axis parallel to the z-axis is studied. When blood flows through a capillary, two phase models emerge: the region of erythrocyte suspension, which is handled as a non-Newtonian power law fluid model, and a Newtonian fluid model for the cell-free layer of plasma. λ be the thickness of the peripheral layer of plasma, π_i is the interstitial fluid pressure, and c0 represents the constant blood concentration in a capillary (Fig. 1). The movement of nanoparticles of concentration c in a capillary is explored under the pressure of a peripheral layer of plasma and a minor slip at the capillary wall.

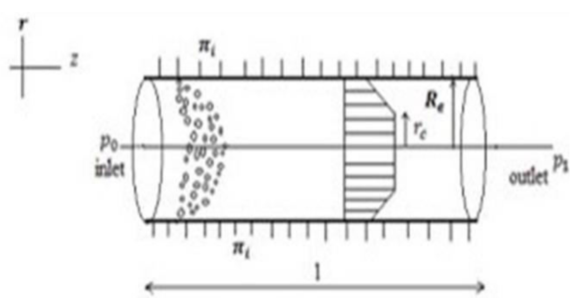

Fig. 1: Nanoparticle movement in blood capillaries over time

Governing Equations:

(i) The Power law fluid expresses the following equation for the central area:

$$\frac{du_1}{dr} = -\left(\frac{1}{2}\frac{P}{\mu_1}\right)^{\frac{1}{n}} r^{\frac{1}{n}}$$

(ii) For the cell- free layer, the consecutive equation is given by--

$$-\frac{\partial p}{\partial z} + \frac{\mu_z}{r}\frac{\partial}{\partial r}\left(r\frac{\partial u_z}{\partial r}\right) = 0$$

$$-\frac{\partial p}{\partial r} = 0$$

(iii) The transport equation along the capillary can be given as--

$$\frac{1}{r}\frac{\partial}{\partial r}\left(r\frac{\partial c}{\partial r}\right) = \frac{u}{D_m}\frac{\partial c}{\partial z}$$

The non-dimensional schemes are

$$Z' = \frac{z}{1}, p' = \frac{p}{\pi_i}, u_1' = \frac{u_1}{u_0}, u_2' = \frac{u_2}{u_0}, \mu_1' = \frac{\mu_1}{\mu_0}, \mu_2' = \frac{\mu_2}{\mu_0}, r' = \frac{r}{R_e}, c' = \frac{c}{c_0}$$

Boundary Conditions of the problem are--

(i) u' is finite at $r' = 0$.

(ii) $u_2' = u_s'$ at $r' = 1$

(iii) $u_1' = u_2'$ at $r' = 1 - \lambda'$

(iv) $\mu_1' \frac{\partial u_1'}{\partial r'} = \mu_2' \frac{\partial u_2'}{\partial r'}$ at $r' = 1 - \lambda$

(v) c' is finite at $r' = 0$

(vi) $c' = 0$ at $r' = 1$

(vii) $c' = 0$ at $r' = 1$

(viii) $\frac{\partial c'}{\partial r'} = 0$ at $r' = 0$

Method of Solution:

The Power Law Fluid Model's constitutive equation is given by

$$\frac{du_1}{dr} = -\left(\frac{1}{2}\frac{P}{u_1}\right)^{\frac{1}{n}} r^{\frac{1}{n}}$$

Now integrating both sides with respect to r, we get,

$$u_1 = -\left({}^1\!/_2\frac{P}{u_1}\right)^{\frac{1}{n}}(r)^{\frac{n+1}{n}}\frac{n}{n+1}+c$$

$$u_1 = -\left({}^1\!/_2\frac{P}{u_1}\right)^{\frac{1}{n}}(r'Re)^{\frac{n+1}{n}}\cdot\frac{n}{n+1}+c\ [\therefore r = r'.Re]$$

Now we use the boundary condition $u_1' = u_2'\ at\ r' = 1-\lambda'$

$$\therefore c = u_2'u_o + \frac{n}{n+1}\left(\frac{1}{2}.\frac{P'}{\mu_1}\right)^{1/n}[(1-\lambda')Re]^{\frac{n+1}{n}}$$

$$or,\quad u_1' = -\left(\frac{1}{2}.\frac{P'}{\mu_1}\right)^{\frac{1}{n}} r^{\frac{n+1}{n}}.\frac{n}{n+1}+u_2'u_o+\frac{n}{n+1}\left(\frac{1}{2}.\frac{P'}{\mu_1}\right).[(1-\lambda')Re]^{\frac{n+1}{n}}$$

$$or,\quad u_1' = u_2'u_o+\frac{n}{n+1}\left(\frac{1}{2}.\frac{P'}{\mu_1}\right)^{1/n}\left[\{(1-\lambda')Re\}^{\frac{n+1}{n}}-r^{\frac{n+1}{n}}\right]$$

$$or,\quad u_1' = u_2'u_o+\frac{n}{n+1}\left(\frac{1}{2}.\frac{P'}{\mu_1}\right)^{\frac{1}{n}}\left[\{(1-\lambda')Re\}^{\frac{n+1}{n}}-r^{\frac{n+1}{n}}\right]$$

$$or,\quad u_1' = \frac{n}{n+1}.\frac{1}{u_o}\left(\frac{1}{2}.\frac{P'}{\mu_1}\right)^{1/n}\left[\{(1-\lambda')Re\}^{\frac{n+1}{n}}-r^{\frac{n+1}{n}}\right]$$

$$or,\quad u_1' = \frac{n}{n+1}.\frac{1}{u_o}\left(\frac{1}{2}.\frac{P'}{\mu_1}\right)^{1/n}\left[(1-\lambda')^{\frac{n+1}{n}}.Re^{\frac{n+1}{n}}-(r'Re)^{\frac{n+1}{n}}\right]$$

$$or,\quad u_1' = \Psi\left(\frac{P'}{2\mu_1}\right)^{1/n}.\frac{n}{n+1}\left[(1-\lambda')^{\frac{1}{n+1}}-r'^{\frac{1}{n+1}}\right]+u_2'$$

$$\left[where\Psi = \frac{Re}{\mu_o}\left(\frac{\pi i}{l}.\frac{Re}{\mu_o}\right)^{\frac{1}{n}}, P' = \frac{dP'}{dz'}\right]$$

The constitutive equation for the cell-free layer is

$$-\frac{\partial P}{\partial z}+\frac{\mu_z}{r}\frac{\partial}{\partial r}\left(r\frac{\partial u_z}{\partial r}\right) = 0$$

Again

$$-\frac{\partial P}{\partial r} = 0\ so\ P = constant$$

Since $P = constant, \frac{\partial P}{\partial z} = 0$

Solving this using boundary layer conditions $u_2' = u_s'\ at\ r' = 1$ and

$\mu_1'\frac{\partial u_1'}{\partial r'} = \mu_2'\frac{\partial u_2'}{\partial r'}\ at\ r' = 1-\lambda$ we get

$$u_2' = u_s'atr = r'and$$

$$\mu_1'\frac{\delta u_1'}{\delta r'} = \mu_2'\frac{\delta u_2'}{\delta r'}atr' = 1-\lambda'weget,$$

$$u_2' = \frac{1}{\mu_2'.A}.\frac{P'}{4}\left(1-r'^2\right)+B_2logr'+\mu_s'$$

$$whereB_1' = \frac{1}{\mu_2'.A}.\frac{P'}{4}(1-(1-\lambda')^2)$$

$$B_2' = \frac{(1-\lambda')}{\mu_2'}\left[\frac{1}{A}P'\frac{(1-\lambda')}{2}-u_1'.\Psi\left(\frac{P'}{2u'}\right)(1-\lambda')^{\frac{1}{n-1}}\right]$$

$$A = \frac{l\mu_o.u_o}{\pi iRe^2}$$

$$u_1 = \Psi\left(\frac{p}{2\mu'}\right)^{1/n}.\frac{n}{n+1}\left[(1-\lambda')^{\frac{1}{n+1}}-r'^{\frac{1}{n+1}}\right]$$

$$+B_1+B_2log(1-\lambda')+u_s'$$

The volumetric flow rate is determined as follows:

$$Q' = Q_1'+Q_2'$$

$$\theta_1' = 2\pi\int_0^{1-\lambda'}u_1'r'dr'$$

$$= 2\pi\int_0^{1-\lambda'}\left[\left(\frac{p}{2u'}\right)^{1/n}.\frac{n}{n+1}\left[(1-\lambda')^{\frac{n+1}{n}}r'-r'^{\frac{1+2n}{n}}\right]\right.$$

$$\left.+B_1r'+B_2r'log(1-\lambda')+r'u_s'\right]$$

$$= 2\pi\left[\left\{\left(\frac{p}{2u'}\right)^{1/n}\Psi.\frac{n}{n+1}\left[(1-\lambda')^{\frac{n+1}{n}}.\frac{r'}{2}-r'^{\frac{1+3n}{n}}.\frac{n}{1+3n}\right]\right.\right.$$

$$\left.+B_1\frac{r'^2}{2}+B_2\frac{r'^2}{2}log(1-\lambda')+\frac{r'^2}{2}u_s'\right]$$

$$Q_1' = \pi(1-\lambda')^2[\Psi\left(\frac{p'}{2u'}\right)^{\frac{1}{n}}.\frac{n(1-\lambda')^{\frac{1}{n+1}}}{1+3n}+B_1+B_2log(1-\lambda')+u_s']$$

Now

$$Q' = Q_1' + Q_2'$$

$$\theta_1{}' = 2\pi \int_0^{1-\lambda'} u_1{}' r' dr'$$

$$= 2\pi \int_0^{1-\lambda'} \left[\left(\frac{p}{2u'}\right)^{1/n} . \frac{n}{n+1} \left[(1-\lambda')^{\frac{n+1}{n}} r' - r'^{\frac{1+2n}{n}} \right] \right.$$

$$\left. + B_1 r' + B_2 r' log(1-\lambda') + r' u_s{}' \right]$$

$$= 2\pi \left[\left\{ \left(\frac{p}{2u'}\right)^{1/n} \Psi . \frac{n}{n+1} \left[(1-\lambda')^{\frac{n+1}{n}} . \frac{r'}{2} - r'^{\frac{1+3n}{n}} . \frac{n}{1+3n} \right] \right. \right.$$

$$\left. + B_1 \frac{r'^2}{2} + B_2 \frac{r'^2}{2} log(1-\lambda') + \frac{r'^2}{2} u_s{}' \right]$$

$$Q_1{}' = \pi(1-\lambda')^2 [\Psi \left(\frac{p'}{2u'}\right)^{\frac{1}{n}} . \frac{n(1-\lambda')^{\frac{1}{n+1}}}{1+3n} + B_1 + B_2 log(1-\lambda') + u'_s]$$

Again

$$u' = \frac{Q'}{\pi} = \frac{Q_1' + Q_2'}{\pi}$$

$$u' = (1-\lambda)^2 [\Psi \left(\frac{p'}{2u'}\right)^{\frac{1}{n}} . r(1-\lambda')^{\frac{1}{n+1}} + B_1 + B_2 log(1-\lambda') + u'_s]$$

$$+ \frac{p'}{u_2' 4A} \left(\frac{1}{2} - (1-\lambda')^2 log(1-\lambda') - \frac{1}{2}(1-\lambda')^4 \right)$$

$$-B_2 \left\{ (1-\lambda')^2 log(1-\lambda') + \frac{1}{2}(1+(1-\lambda')^4) \right\} + u_s'(1-(1-\lambda')^2)$$

For r'=0, the concentration c' is expressed as a result of solving the equation $\frac{1}{r}\frac{\partial}{\partial r}\left(r\frac{\partial c}{\partial r}\right) = \frac{u}{D_m}\frac{\partial c}{\partial z}$ using boundary conditions $c' = 0$ at $r' = 1$ and $c' = 0$ at $r' = 1$, are given on taking $D_m' = D_m \frac{1}{u_0 R_s^2}$

$$c'(r') = \frac{1}{D_m}\frac{\partial c'}{\partial z'} \left[\left\{ \Psi \left(\frac{p}{2\mu_1{}'}\right)^{1/n} \frac{n}{2(3n+1)} (1-\lambda')^{\frac{1}{n}+3} + B_1 \frac{(1-\lambda')^2}{2} + B_2 \frac{(1-\lambda')^2}{2} log(1-\lambda') \right. \right.$$

$$\left. + u_s{}' \frac{(1-\lambda')^2}{2} \right\} logr'$$

$$+ \left\{ \frac{1}{\mu_2{}' A} \frac{p'}{4} \left(\frac{r'^2}{4} - \frac{r'^4}{16} - \frac{(1-\lambda')^2}{2} logr' + \frac{(1-\lambda')^4}{4} logr' - \frac{3}{16} \right) + B_2 \left(\frac{r'^2}{4} logr' \right. \right.$$

$$\left. - \frac{r'^2}{8} - \frac{(1-\lambda')^2}{2} logr' . log(1-\lambda') + \frac{(1-\lambda')^2}{4} logr' + \frac{1}{8} \right)$$

$$\left. \left. + u_s{}' \left(\frac{r'^2}{4} - \frac{(1-\lambda')^2}{2} logr' - \frac{1}{4} \right) \right\} \right]$$

Results and Discussion

To offer an estimate of their qualitative and quantitative effects, the physical and rheological features involved in the analysis must be quantified. The values for various material constants and other parameters were obtained from established literatures. The graphs are plotted and computer codes are created.

Figure 2 denotes the behaviour of u' vs r' for varying λ'. Here we see the velocity profile increases as the peripheral layer increases. The velocity profile is a straight line throughout the peripheral layer. It also increases with r'.

Figure 3 denotes the behaviour of u' vs r' for varying n. In this case, we see that the velocity profile is linear in nature. But its nature changes with the flow behaviour index. Velocity profile decreases with increasing n. When n=0.85 the velocity profile is abrupt. It increases till r' = 0.6 and decreases. For the other values of n velocity profile increases linearly.

Figure 4 denotes the behaviour of u' vs r' for varying $u_s{}'$. The velocity profile is linear, increasing with increasing r'. But it does not vary with the change in slip velocity.

Figure 5 denotes the behaviour of u' vs r' for varying P'. Velocity profile is linear and increases with increase in r'. It also increases with P'.

Figure 6 denotes the behaviour of c' vs r' for varying λ'. The concentration of nanoparticles drops linearly as the capillary radius increases. It also decreases with increasing values of λ'.

Figure 7 denotes the behaviour of c' vs r' for varying n. The relationship is linear and the value of c' decreases with increasing values of n.

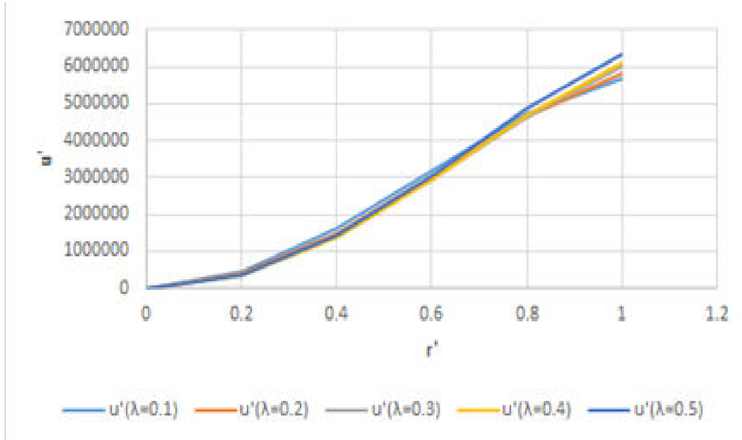

Fig. 2: u' vs r' for varying λ'.

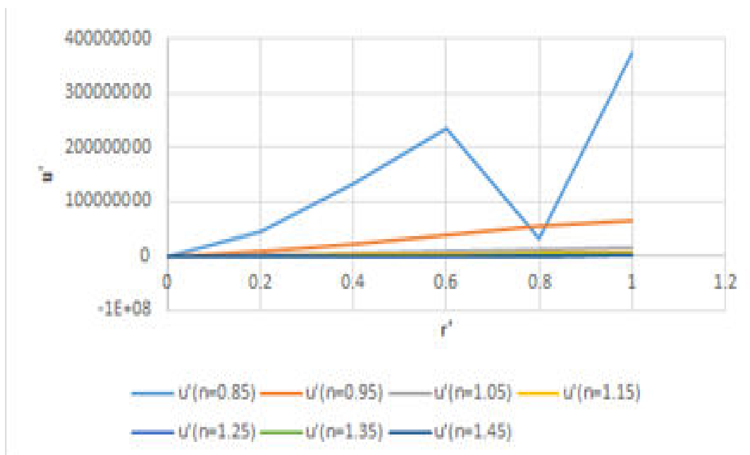

Fig. 3: u' vs r' for varying n.

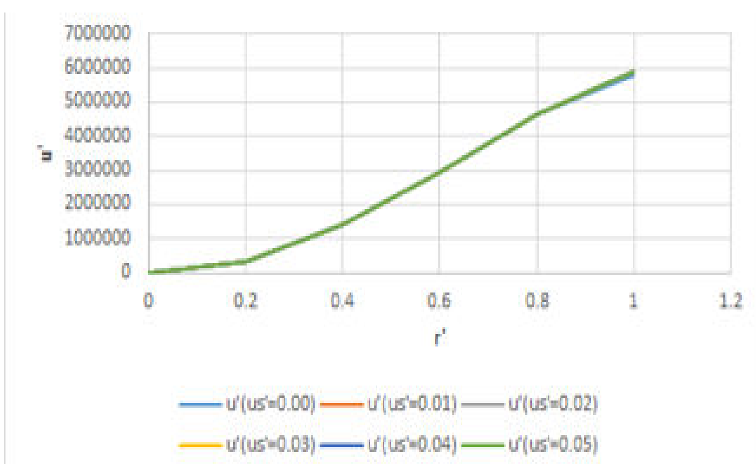

Fig.4: u' vs r' for varying u_s'.

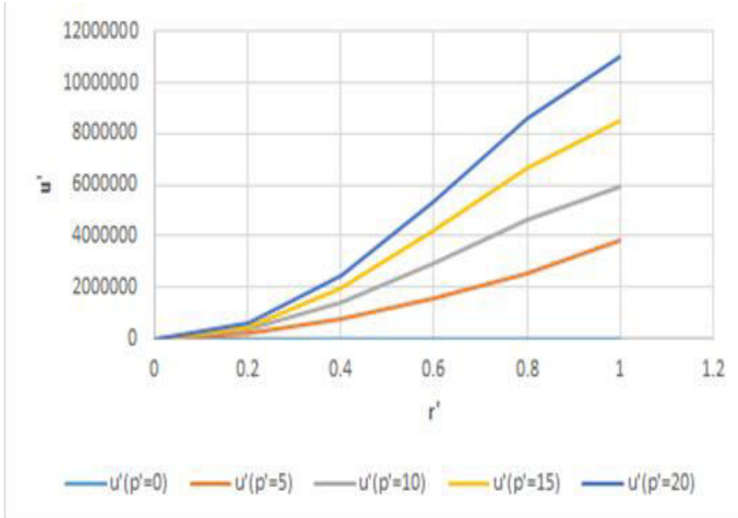

Fig. 5: u' vs r' for varying P'.

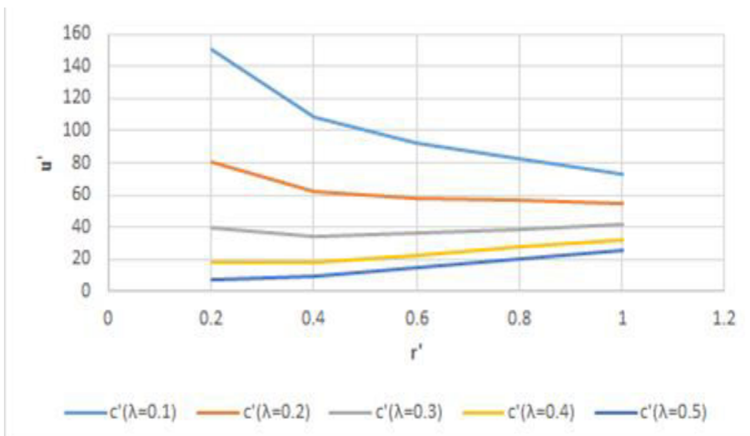

Fig. 6: c' vs r' for varying λ'.

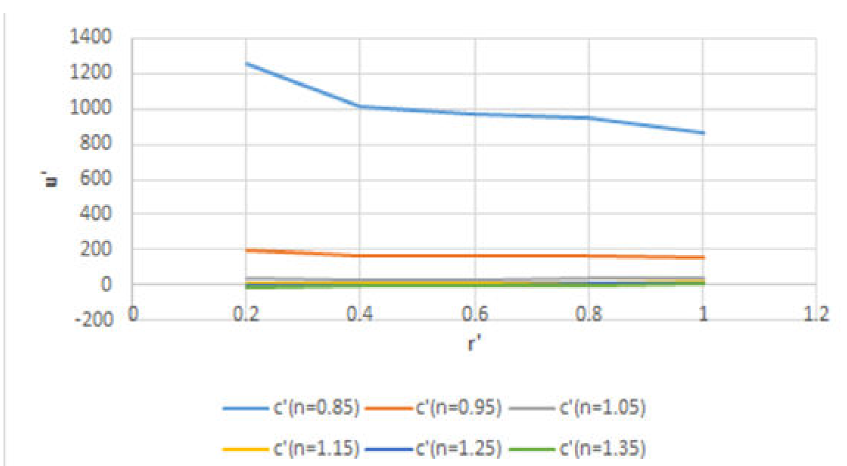

Fig. 7: c' vs r' for varying n.

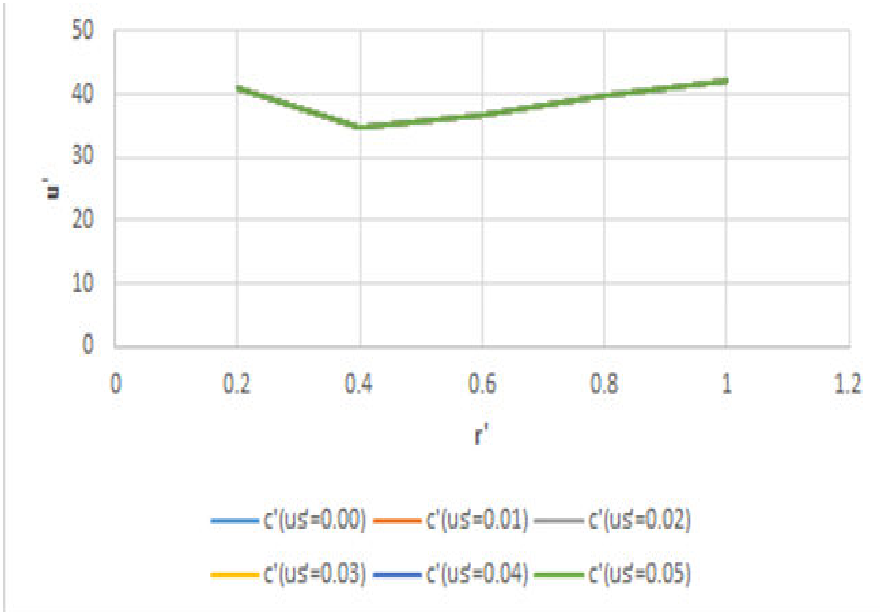

Fig. 8: c' vs r' for varying $u_s{}'$.

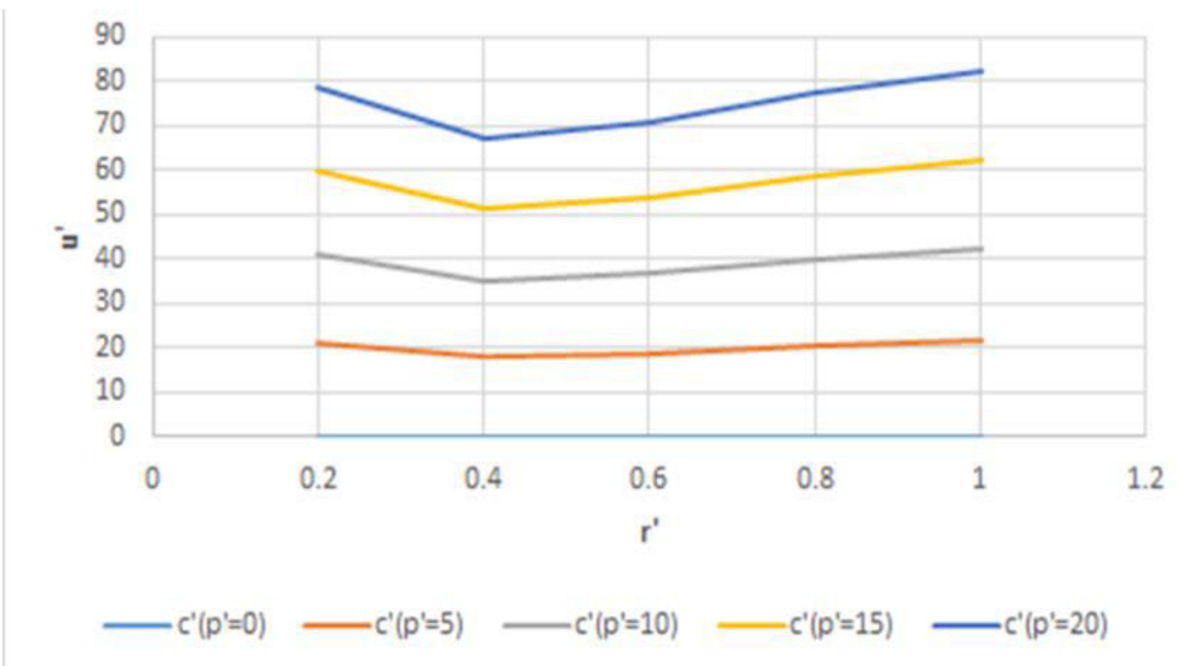

Fig. 9: c' vs r' for varying P'.

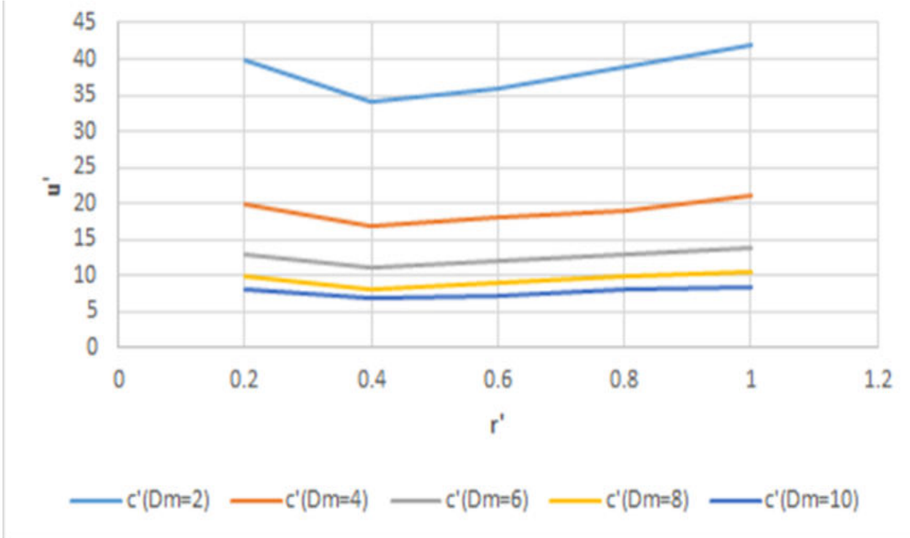

Fig. 10: c' vs r' for varying Dm.

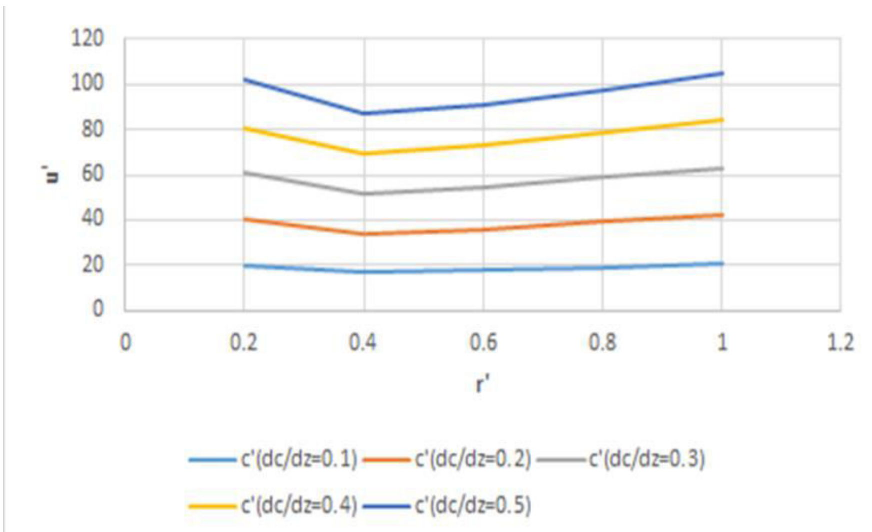

Fig. 11: c' vs r' for varying $-\frac{\partial c}{\partial z}$.

Figure 8 denotes the behaviour of c' vs r' for varying slip velocity $u_s{}'$. The concentration does not vary with slip velocity but it decreases till r'=0.4 and increases for r' > 0.4.

In Figure 9 the behaviour of c' vs r' for varying P' is shown. It decreases with increasing P' and follows a linear relationship.

Figure 10 denotes the behaviour of c' vs r' for varying Dm. The value of c' again decreases with increasing Dm. The relationship is linear.

Figure 11 denotes the behaviour of c' vs r' for varying $-\frac{\partial c}{\partial z}$. In this case the concentration of nanoparticles increases with increasing $-\frac{\partial c}{\partial z}$. The relationship is linear.

From the above analysis it can be seen that the velocity profile and concentration of nanoparticles are varying with the change of other properties of the blood. In most cases they are varying linearly with the radius of capillary.

Conclusion

Capillary rheology and blood flow dynamics are significant not only because capillaries are the major location of oxygen and nutrient exchange, but also because the rheological behaviour of Red Blood Cells (RBCs) in these veins determines optimal microcirculatory function. Due to the high-volume proportion (approximately 99 per cent) of RBCs in blood cells, blood can be seen in capillaries as a suspension of RBCs in plasma. The organisation, orientation, and deformability of RBCs in plasma suspension have been found to have a considerable impact on capillary flow dynamics. The research contributes to a better knowledge of the dynamic properties of blood flow in capillaries. This research could be used to investigate various medical disorders, such as sickle cell disease (SCD), which causes RBCs to become hard, pointed, and sticky, forming crescents or sickles. This model could potentially be used to predict microscopic hemodynamic and hemorheological behaviours in more complicated microcirculation scenarios, such as curved and stenotic micro-vessels, branching, and post-capillary expansions.

References

Caro CG, Fitz-Gerald JM and Schroter RC. (1971) Atheroma and arterial wall shear. Observation, correlation and proposal of a shear dependent mass transfer mechanism for atherogenesis. Proc R Soc Lond B Biol Sci. 177(1046):109-159.

Charm S and Kurland G. (1965) Viscometry of human blood for shear rates of 0-100,000 sec-1. Nature 206(984): 617-618.

Ellahi R, Rahman SU, Nadeem S and Akbar NS. (2014) Blood flow of nanofluid through an artery with composite stenosis and permeable walls. Appl Nanosci. 4: 919-926.

Gentile F, Ferrari M and Decuzzi P. (2008) The transport of nanoparticles in blood vessels: the effect of vessel permeability and blood rheology. Ann Biomed Eng. 36(2): 254-261.

Kirkeeide RL, Young DF and Cholvin NR. (1977) Wall vibrations induced by flow through simulated stenosis in models and arteries. J Biomech. 10(7): 431-441.

Lee JS. (1974) On the coupling and detection of motion between an artery with a localized lesion and its surrounding tissue. J Biomech. 7(5): 403-409.

Mekheimer K S and El Kot MA. (2012) Mathematical modeling of unsteady flow of a Sisko fluid through an isotropically tapered elastic arteries with time-variant overlapping stenosis, App Math Model. 36: 5393.

Misra JC and Shit GC. (2007) Role of slip velocity in blood flow through stenosed arteries: A Non- Newtonian model. J Mech Med Biol. 7(3): 337-353.

Mostafa AAM. (2011) Slip velocity effect on a non-Newtonian power-law fluid over a moving permeable surface with heat generation. Math Compu Modell. 54: 1228-1237.

Priyadharshini S and Ponalagusamy R. (2015) Biorheological model on flow of Herschel-Bulkley fluid through a tapered arterial stenosis with dilatation. Appl Bionics Biomech. 2015: 406195.

Revellin R, Rousset F, Baud D and Bonjour J. (2009) Extension of Murray's law using a non-Newtonian model of blood flow. Theor Biol Med Model 6: 7.

Sandeep S and Shine SR. (2021) Effect of stenosis and dilatation on the hemodynamic parameters associated with left coronary artery. Comput Methods Programs Biomed. 204: 106052.

Shukla JB, Gupta SP and Parihar RS. (1980) Biorheological aspects of blood flow through artery with mild stenosis: effects of peripheral layer. Biorheology 17(5-6): 403-410.